



THERMAL- AND STRAIN-RELATED BEHAVIOUR OF A SHAPE MEMORY ALLOY UNDER EARTHQUAKE LOADING CONDITIONS

M. J. Wesolowsky¹ and J. C. Wilson²

ABSTRACT

This paper presents results from work on the hysteretic modelling of shape memory alloy (SMA) materials for applications in earthquake engineering and their use in controlling the response of single-degree-of-freedom (SDOF) systems subjected to earthquake ground motions.

One of the more widely-used behavioural models in seismic applications of SMAs is the Wilde, Gardoni and Fujino (WGF) model. This model however does not consider the effects of operating (ambient) temperature, strain rate (which is linked to temperature effects) and strain amplitude. These factors can considerably affect the damping capacity of a structural system that uses SMA-based devices for seismic control. In this work, the WGF model has been extended to numerically include the effects of operating temperature, strain rate and strain amplitude. This model is shown to be capable of closely replicating the hysteresis behaviour observed in laboratory tests of SMA materials under simulated seismic loading conditions.

A study on SMA-based SDOF systems has shown that by varying the ambient temperature of the system, the maximum seismically-induced stresses predicted by the extended WGF model can be more than 50% higher than those predicted by the original model that does not include the effects of temperature, strain rate and strain amplitude. The maximum strains predicted by the extended model range from -20 to +20% of the values predicted by the original model, and energy dissipation calculated from the extended model is shown to be substantially below the levels predicted when these effects are not taken into account.

Introduction

Shape memory alloys (SMAs) (Funakubo 1987) are a class of alloys that have the capability to dissipate energy through repeated cycling loading without significant permanent deformations. They have an unusually high usable strain range compared to other metals, as shown in Figure 1. The most common SMA used for seismic application is NiTi (commonly referred to as Nitinol), which is composed of approximately equal proportions of nickel and

¹Senior Engineer, Rowan Williams Davies & Irwin (RWDI) Inc, Consulting Engineers and Scientists, Guelph, ON N1K 1B8

²Professor, Dept. of Civil Engineering, McMaster University, Hamilton, ON L8S 4L7

titanium. Wilson and Wesolowsky (2005) provide a detailed presentation on aspects of the material behaviour of SMA material.

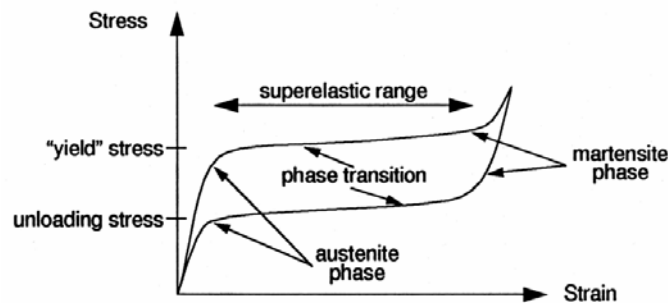


Figure 1 General form of shape memory alloy superelastic behaviour (Clark et al. 1995).

One popular hysteretic behavioural model for SMAs was proposed by Wilde, Gardoni & Fujino (WGF) (2000), based on a model developed by Graesser & Cozzarelli (1991). This model, which considers only mechanical loading under isothermal conditions, captures both the superelastic range and the martensitic hardening characteristics of SMAs, which are critical for 'fail-safe' action for extreme loads. Readers are directed to the original publication by Wilde, Gardoni & Fujino (2000) for a detailed description of the WGF model. Wesolowsky & Wilson 2006, have extended the WGF model to include the effects of: (1) ambient (operating) temperature, (2) strain rate (loading frequency), and (3) strain amplitude. This paper presents a study of Single-Degree-of-Freedom (SDOF) systems that use the extended WGF model to demonstrate the impact of including these effects, and how critical they can be to properly predict the strain, stress and energy dissipation capacity of SMA seismic isolators.

Limitations of the WGF Model for Shape Memory Alloy Hysteresis

The WGF model does not consider the effects of three seismically-induced dynamic characteristics. This section outlines the effect of ambient (operating) temperature, strain rate (loading frequency), and strain amplitude on the observed experimental hysteretic response of Nitinol.

Temperature Effects

Since the behaviour of SMAs is highly dependent on the transition temperatures of the material, so too does the operating (ambient environment) temperature influence the hysteretic behaviour of the material. Dolce & Cardone (2001) studied the effects of operating temperature on NiTi wires in tension and showed that as the ambient temperature increases, the hysteretic loops are shifted upward. The relationship between the transformation stresses and the ambient temperature is linear, in this case approximately $6 \text{ MPa}/^\circ\text{C}$. It was also shown that the equivalent damping decreased from 13% to 8% as the temperature increased.

Strain Rate Effects

SMA's can produce large amounts of heat during rapid cyclic loading, which at times can be difficult to dissipate, depending on the arrangement of SMA material in the device (e.g., size of device, physical characteristics and confinement of the SMA material). Since SMA's are particularly sensitive to the temperature of operation, significant changes in behaviour can be noticed for temperature shifts during operation, which can be a direct result of the frequency of loading, through the increase of material temperature (Piedboeuf et al. 1998). Dolce & Cardone (2001) studied the effects of loading frequency on NiTi wires in tension. Experimental testing indicated that equivalent damping decreased from 9% for 0.02 Hz (quasi-static) to 6.5% for 4 Hz.

Strain Amplitude Effects

Dolce & Cardone (2001) noted that for higher strain amplitudes, the stress at which the reverse phase transformation begins occurs at lower levels. This has the effect of increasing the damping capacity of the device for larger strain amplitudes, and can have a direct bearing on the seismic response of a system isolated with SMA dampers. A sample loaded at increasing strains from 1.5 to 7.5% caused the equivalent damping to increase from 2% to 7.5%.

Extending the WGF Model

Since the material temperature (due to ambient temperature and strain rate) and the maximum strain amplitude will vary during a given seismic input, the path that the stress-strain behaviour will follow will constantly shift. However, the existing WGF model will produce only one specific hysteretic loop. Therefore what must be considered is to replace the five model constants (see Wilde, Gardoni & Fujino 2000) with variable expressions, linked to the ambient temperature, strain rate and strain amplitude for a given time-step.

The overall approach to extension of the model involves fitting a series of individual hysteretic curves to existing data, with each curve being for a different combination of ambient temperature and maximum strain amplitude. Each fitted curve using the WGF model requires a set of parameter values to produce the necessary size and shape of loop to match experimental data. By carrying out this procedure for a range of temperatures and strain amplitudes, variable expressions for each model parameter will be produced that will be functions of temperature and strain amplitude. Due to space limitations, the authors refer the reader to Wesolowsky & Wilson (2006) for a detailed description of the extension methodology.

This method requires experimental data, providing relationships between hysteretic behaviour, operating temperature and maximum strain amplitude. The work of Dolce & Cardone (2001) is one of the most complete experimental characterizations available in the literature and parameter variable expressions developed from their superelastic experimental data have been implemented into an extended WGF model.

Implementation of the Extended WGF Model

The figures in this section show a series of response prediction comparisons between the extended and original WGF models based on the effects of varying the ambient temperature conditions. The effects of strain amplitude have been intrinsically built into each comparison (through the nature of the extended model).

Examples of SMA Seismic Responses to Individual Ground Motions

Figures 2a-e show the predicted hysteretic behaviour of a SMA-based SDOF system using the extended WGF model with ambient temperatures of 10°C, 15°C, 20°C, 25°C and 30°C. These predictions were computed using the fault-normal component of the Yarımcı record of the Kocaeli, Turkey (1999) earthquake scaled to a maximum pgv of 40 cm/s and an assumed inherent damping of 5% (separate from the damping provided by the SMA material). The austenitic stiffness of the system produces an initial ‘elastic’ period of 0.3 seconds. The hysteretic behaviour computed using the original WGF model is also shown in Figures 2a-e, corresponding to an ambient temperature of 10°C and quasi-static loading conditions.

Figure 2a illustrates that at 10°C, the extended model predicts a maximum strain and corresponding stress that is nearly identical to that predicted by the original model (with the ‘compression’ side of the response showing slightly lower magnitudes for the original model). The hysteretic behaviour however, has obvious differences, with the extended model producing noticeably thinner loops, especially on the ‘tension’ side of the axis. Figure 2b shows that at an ambient temperature (considered by the extended model) of 15°C the superelastic stress plateau is higher than in the original model (where the data is for the 10°C condition). This trend continues as ambient temperature rises, where in Figure 2e the behaviour of the extended model appears to be almost entirely austenitic in nature (the superelastic plateau never fully develops).

Figure 2f summarizes the normalized maximum strains and stresses in the SMA material predicted for the five ambient operational temperatures considered in Figures 2a-e. The values on this plot have been calculated by dividing the maximum responses (and energy dissipated) at each temperature by those obtained at 10°C (using the extended WGF model), thus resulting in a value of 1 for an ambient temperature of 10°C. As demonstrated in Figures 2a-e, increasing the ambient temperature of loading produces extended model predictions of lower maximum strains (-8% at 30°C) and higher maximum stresses (+30% at 30°C). Since the extended model captures more of the austenitic hysteretic behaviour the dissipated energy is reduced by 80%.

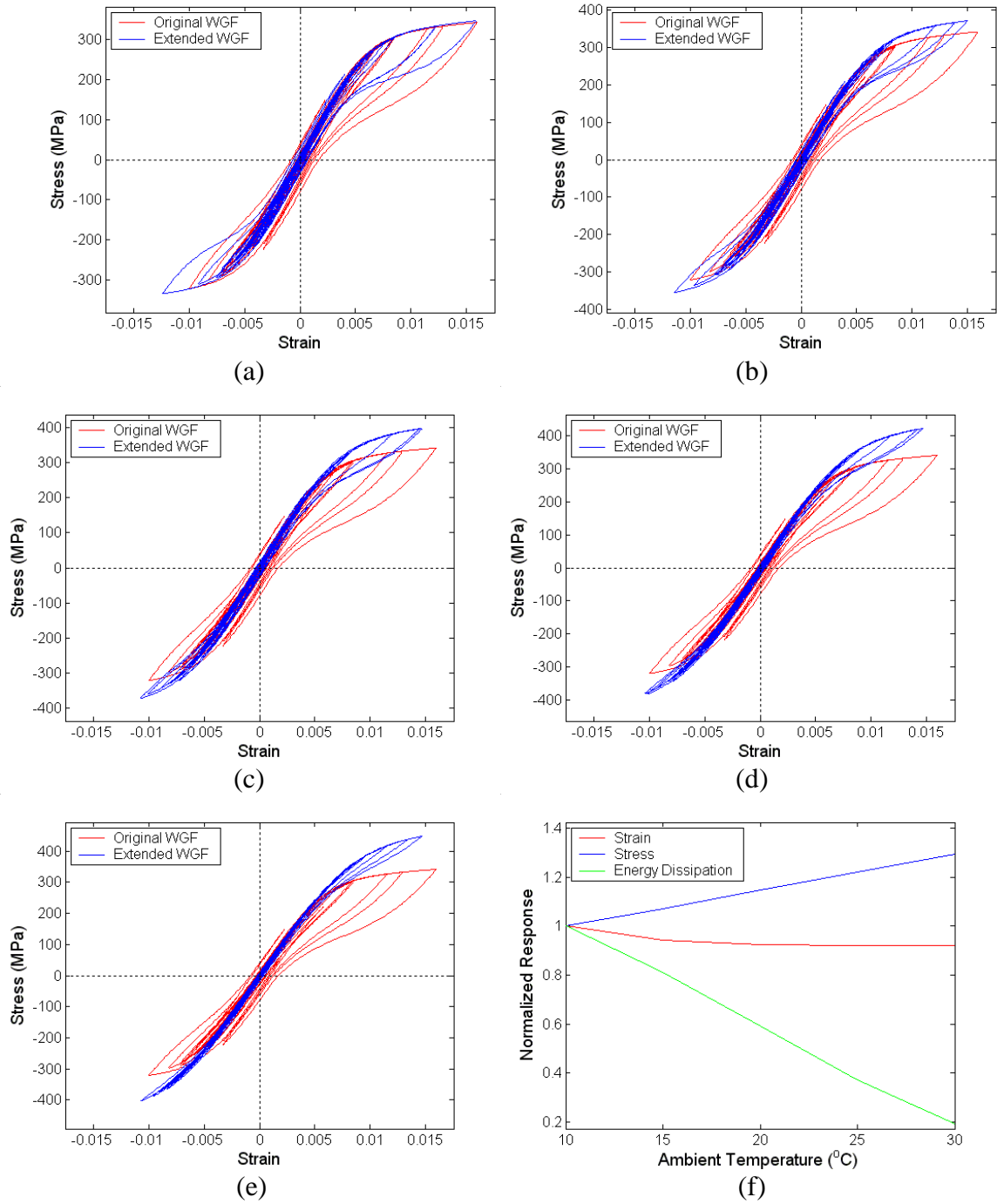


Figure 2 (a) – (e) Hysteretic behaviour of a SMA SDOF system for ambient temperatures of 10°C, 15°C, 20°C, 25°C and 30°C using the Yarımcı record of the Kocaeli, Turkey (1999) earthquake scaled to a maximum pgv of 40 cm/s, and austenitic stiffness producing an initial period of 0.3 seconds; (f) the effect of ambient temperature on normalized SDOF responses.

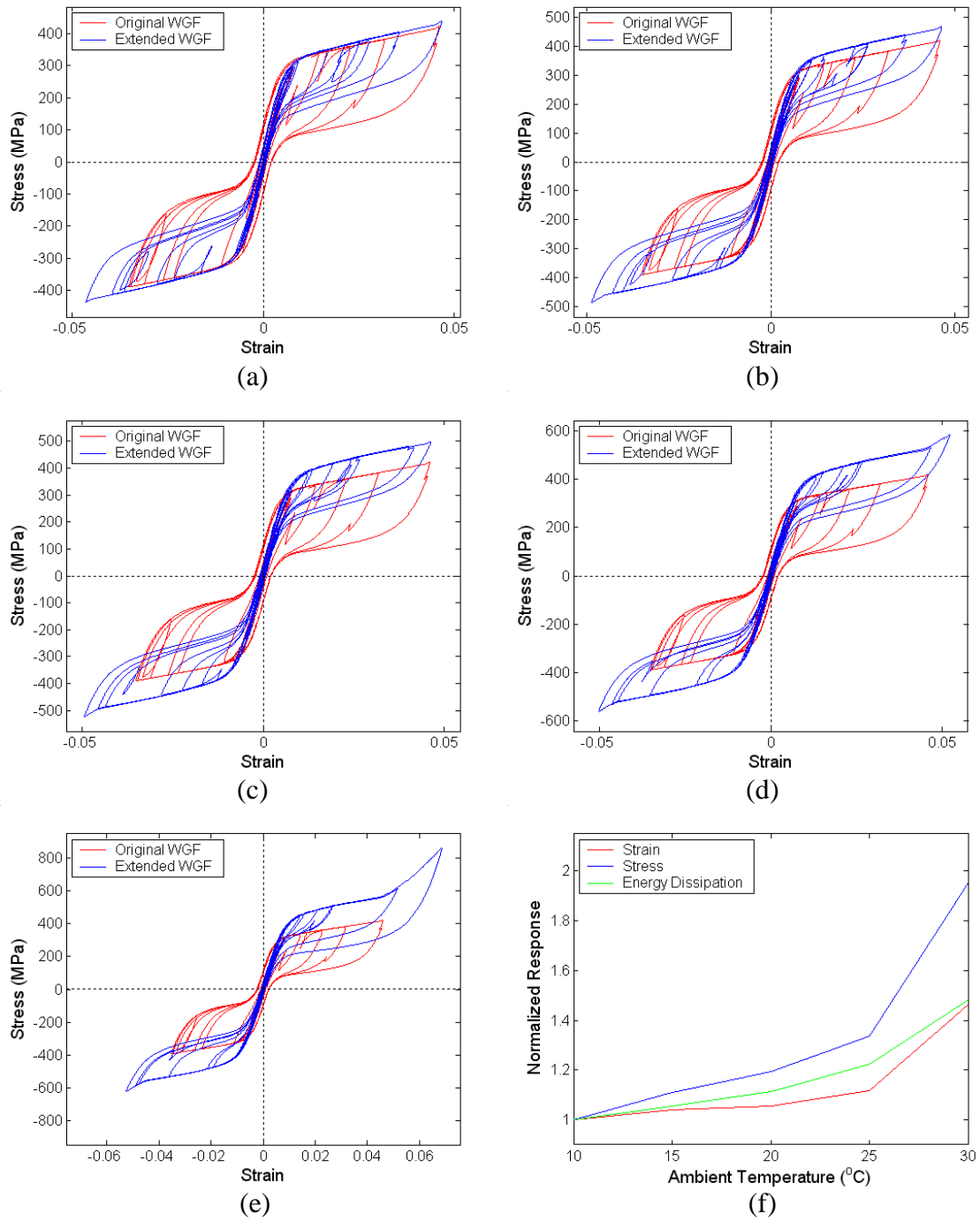


Figure 3 (a) – (e) Hysteretic behaviour of a SMA SDOF system for ambient temperatures of 10°C, 15°C, 20°C, 25°C and 30°C using the Stone Canyon record of the Northridge (1994) earthquake scaled to a maximum pgv of 40 cm/s, and austenitic stiffness producing an initial period of 1.05 seconds; (f) the effect of ambient temperature on normalized SDOF responses.

Figure 3 presents the hysteretic responses for an isolated SDOF system using the Stone Canyon record (Northridge, 1994) scaled to a maximum pgv of 40 cm/s. The austenitic stiffness of the system would produce an initial period of 1.05 seconds, which results in considerably higher strain predictions than those for Figure 2. Figure 3a shows that the extended model predicts maximum strains and stresses that are almost identical to the original model, although again with noticeably different hysteretic behaviour. Figures 3b-e show that as the ambient temperature increases, the maximum strains of the system also increase, which is quite different than the behaviour seen in Figure 2. This is due to a combination of the dynamic characteristics of the earthquake excitation (periods at which the record has the most energy), and the constantly shifting equivalent period of the SDOF system. When the equivalent period of the SDOF is similar to the range where the earthquake contains its greatest energy, dynamic amplification tends to occur, which causes the SDOF to be driven to much greater responses.

Figure 3f summarizes the normalized maximum responses seen in Figures 3a-e. As ambient temperature increases, the maximum strains, maximum stresses and dissipated energy all increase. The maximum strain has increased by just over 45%, while the maximum stress has increased by almost 95%. The dissipated energy of the system increases by almost 50%, even though the hysteretic damping of the SMA material has declined considerably (hysteretic damping decreases as the loops shift upwards – see Dolce & Cardone 2001). This plot highlights the sensitivity that SMAs have towards ambient temperature, and emphasizes that conducting laboratory experiments in order to fit a model must be carried out at a range of ambient temperatures that might be expected during field loading.

Mean Seismic Responses

This section summarizes the behaviour of a SDOF system over a wide range of dynamic properties, subjected to 10 fault-normal components of near field earthquakes at two velocity scalings (pgv=20 and 40 cm/s). It is a compilation of a series of individual responses similar to those presented in Figures 2 and 3. A range of SDOF systems have been considered having initial periods from 0.05 to 2 seconds. The maximum responses (strain, stress) have been recorded from the ten earthquakes considered. Each individual case has been computed using the original WGF model and the extended model. The maximum responses from the extended model have been divided by the maximum responses from the original WGF model, and the means of these ratios have been plotted for each initial period.

Figure 4 shows the comparison of predicted mean of the normalized maximum strains and stresses for both models. Using the extended model results in mainly higher strain predictions across the entire range of initial periods for the 20cm/s scaled earthquakes. The largest differences occur in the range of 0.3 to 1.5 seconds, where the extended model produces strains as high as 20% greater than the original model. This represents the range of responses that occur when the hysteretic behaviour remains mainly below the martensitic hardening strain. It is in these cases where the greatest differences can be seen between the original and the extended models.

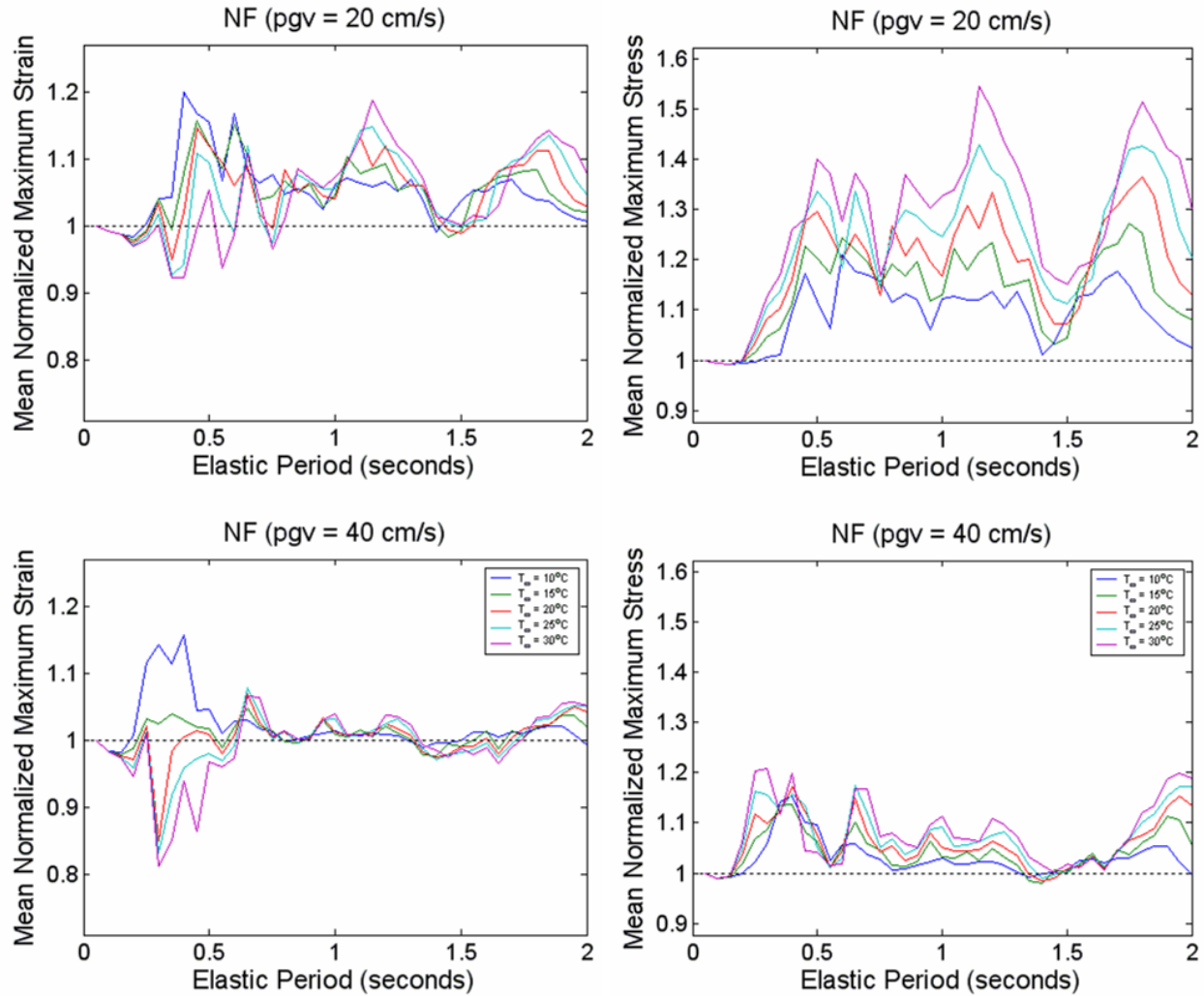


Figure 4 Mean normalized maximum strain and stress predictions for a set of 10 near field earthquakes (fault-normal components only) scaled to 20 and 40 cm/s, for ambient temperatures of 10°C, 15°C, 20°C, 25°C and 30°C.

For lower periods, as ambient temperature increases, the predicted strains decrease, at some periods to levels as much as 20% below the predicted strains using the original WGF model (for the 0.40cm/s scaled earthquakes). This occurs only when the overall strains in the system are relatively low (reaching slightly into the superelastic range). At these relatively low strains, the extended model predicts that the system will remain more in the austenite range than the original model. Thus the decrease in strain predictions for the extended model can be attributed to an overall more rigid system at higher ambient temperatures (as the superelastic range occurs at a higher stress level). This can be seen in Figure 2.

At higher periods, the reverse is seen, where increased ambient temperature result in higher strain predictions. This is due to the system straining predominantly into the superelastic and martensitic hardening ranges. In these cases, the extended model predicts significantly lower values of hysteretic damping (as the loops shift upwards – especially in the martensitic

range due to no further energy dissipation), thus the system is pushed to greater strain values due to its increasing equivalent stiffness and inability to absorb as much energy as the original WGF model predicted.

Figure 4 also illustrates the corresponding stress response comparisons. For almost every period and for both scalings, the stress increases as a result of increasing ambient temperature. This is directly due to the upwards shift in hysteretic behaviour as a result of increased ambient temperature.

The energy dissipated (area inside the hysteretic loops) by the system is greatly affected by ambient temperature, and strain amplitude. Figure 5 showing the mean normalized dissipated energy is consistently less for the extended model than for the original model. The dissipation comparisons at initial periods below 0.2 seconds show that the extended and original models predict identical values of energy dissipation. Both models predict strains that remain entirely within the austenitic range at very low periods, and thus result in no energy dissipation for either model. For periods between 0.2 and 0.7 seconds, the discrepancy between the extended and the original models appears to be the greatest, but this is due to the low amplitude response at these levels, which tend to amplify the differences between low values of energy dissipation.

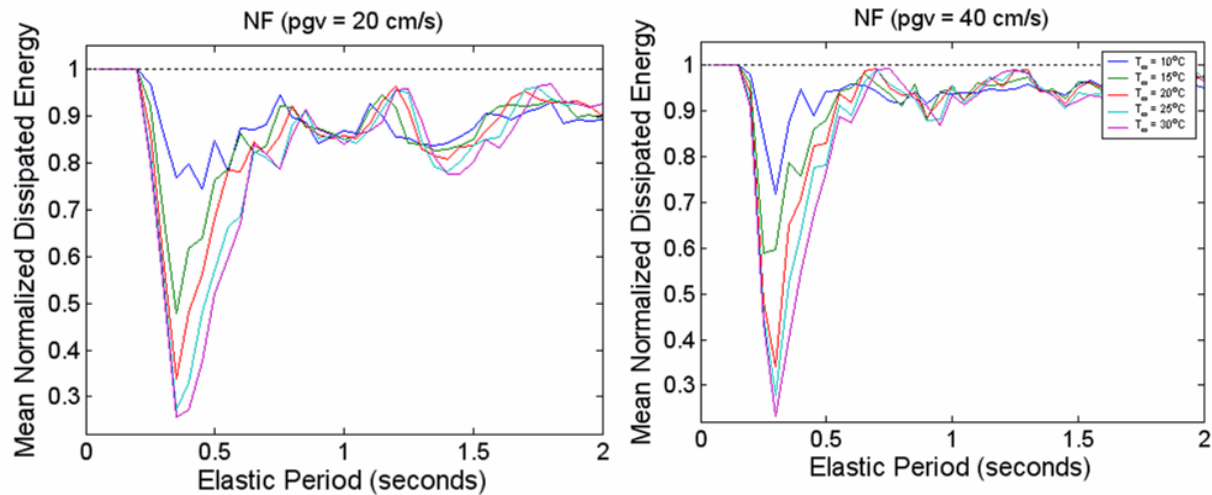


Figure 5 Mean normalized maximum energy dissipated predictions for a set of 10 near field earthquakes (fault-normal components only) scaled to 20 and 40 cm/s, for ambient temperatures of 10°C, 15°C, 20°C, 25°C and 30°C.

The effect of increasing ambient temperature generally has the effect of lowering the predicted energy dissipation capacity of the system. This discrepancy is greatest during the period range where the system barely reaches into the superelastic range. As ambient temperature increases, the hysteretic loops shift upwards, and become thinner for the extended model. This discrepancy becomes smaller as the system reaches the martensitic range.

Conclusions

This study has shown the importance of including the thermal- and strain-related behaviour into the hysteretic model for SMA material when it is used in the high strain-rate loading that accompanies earthquake response. The maximum seismically-induced stresses predicted by the extended WGF model can be more than 50% higher than those predicted by the original model that does not include the effects of temperature, strain rate and strain amplitude. The maximum strains predicted by the extended model range from -20 to +20% of the values predicted by the original model and the energy dissipation capacity predicted by the extended model has been shown to be less than what would be predicted by the model that excludes the thermal and strain-rate dependency.

Acknowledgments

The research support of the Natural Sciences and Engineering Research Council of Canada, and the experimental data provided by M. Dolce and D. Cardone are gratefully acknowledged.

References

- Clark, P.W., I.D. Aiken, J.M. Kelly, M. Higashino, and R.C. Krumme, 1995. Experimental and Analytical Studies of Shape Memory Alloy Dampers for Structural Control, *Proceedings of SPIE – The International Society for Optical Engineering, Smart Structures and Materials, Passive Damping*, San Diego, CA, March 1-2; 2445, 241-251.
- Dolce, M., and D. Cardone, 2001. Mechanical Behaviour of Shape Memory Alloys for Seismic Applications: 2. Austenite NiTi Wires Subjected to Tension, *International Journal of Mechanical Sciences*, 43 (11), 2657-2677.
- Funakubo, H., 1987. *Shape Memory Alloys*, Gordon and Breach Science Publishers, New York, NY.
- Graesser, E.J., and F.A. Cozarelli, 1991. Shape-Memory Alloys as New Materials For Aseismic Isolation, *Journal of Engineering Mechanics*, 117 (11), 2590-2608.
- Piedboeuf, M. C., R. Gauvin, and M. Thomas, 1998, Damping behavior of shape memory alloys: strain amplitude, frequency and temperature effects, *Journal of Sound and Vibration*, 214 (5), 885-901.
- Wesolowsky, M.J., and J.C. Wilson, 2006. Hysteresis Modelling of Shape Memory Alloys for Seismic Engineering Applications, *Proceedings of the 8th U.S. National Conference on Earthquake Engineering*, San Francisco, CA, April 18-22.
- Wilde, K., P. Gardoni, and Y. Fujino, 2000. Base Isolation System with Shape Memory Alloy Device for Elevated Highway Bridges, *Engineering Structures*, 22 (3), 222-229.
- Wilson, J.C., and M.J. Wesolowsky, 2005. Shape Memory Alloys for Seismic Response Modification: A State-of-the-Art Review, *Earthquake Spectra*, 21 (2), 569-601.